Alexandria Engineering Journal (2022) xxx, xxx–xxx

HOSTED BY

ELSEVIER

Alexandria University

Alexandria Engineering Journal

www.elsevier.com/locate/aej
www.sciencedirect.com

Effect of upstream deflector utilization on H-Darrieus wind turbine performance: An optimization study

Iham F. Zidane [a,*], Hesham M. Ali [a], Greg Swadener [b,*], Yehia A. Eldrainy [a,c], Ali I. Shehata [a]

[a] *Mechanical Engineering Department, College of Engineering and Technology, Arab Academy of Science, Technology and Maritime Transport (AASTMT), 1029 Abu Kir, Alexandria, Egypt*
[b] *School of Engineering and Applied Science, Aston University, Aston Triangle, Birmingham B4 7ET, United Kingdom*
[c] *Mechanical Engineering Department, Faculty of Engineering, Alexandria University, Alexandria, Egypt*

Received 6 September 2021; revised 19 July 2022; accepted 23 July 2022

KEYWORDS

H-Darrieus;
Vertical Axis Wind Turbine;
Deflector;
Aerodynamic performance;
CFD

Abstract This paper aims to enhance the performance of H-Darrieus Vertical Axis Wind Turbine (VAWT) via introducing upstream deflectors. The impact of this addition has been investigated and discussed through different deflector configurations. The turbine performance before and after adding different wind rotor barriers was compared. A two dimensional, incompressible, transient, and turbulent flow model was built up in order to simulate the air flow around the turbine blades. Model verification and validation were performed through comparing the model solutions using different mesh sizes, time steps, turbulent models, and discretization schemes. Computational Fluid Dynamics (CFD) models were validated to provide novel insights on the effect of the deflectors on the aerodynamic characteristics of a VAWT blades. Results showed that the presence of a single deflector increases the highest value of the moment coefficient of the bare configuration by 24%, either increases the negative torque values, while two defectors increase the maximum value by 22% and the overall average value of the moment coefficient over the optimal range for the tip speed ratio.

1. Introduction

Wind energy is one of renewable energy sources because of its low environmental impact and cost effectiveness [1,2]. It supplies 2.3 % of the total world's electrical power [3] and is estimated to increase to 22 % by the 2030 [4]. Vertical Axis Wind Turbines (VAWTs) are becoming important in wind power

* Corresponding authors.
E-mail addresses: iham_zidane@aast.edu (I.F. Zidane), j.g.swadener@aston.ac.uk (G. Swadener).

Peer review under responsibility of Faculty of Engineering, Alexandria University.

https://doi.org/10.1016/j.aej.2022.07.052

Nomenclature

c	cord length	V	wind velocity
Cm	Moment Coefficient	α	angle of attack
Cp	Coefficient of performance	ω	Angular speed
D	rotor diameter	λ	Tip speed ratio
H	rotor height	λ	Tip speed ratio
L	reference length	σ	Rotor Solidity
N	number of blades	$\varnothing$	azimuth angle
R	turbine radius		
t	Time Step		

generation due to its compactness and adaptability for domestic installations. In contrast, it is well known that VAWTs have lower efficiency compared to Horizontal Axis Wind Turbines (HAWTs) [1]. Researchers and wind turbine industries are trying to optimize the VAWT rotor designs to improve their performance. Some numerical codes, such as vortex model or multiple stream tube model, have been established for VAWT performance predictions and efficiency optimization. However, these codes are based on 1D simplified equations and accurate aerodynamic experimental data for the required airfoils [5]. Previous research shows that there are two ways utilized to reach the goal of maximizing the power generated from wind turbines. The first way is to apply some modifications on the initial wind turbine design, and the second one is to insert a power augmentation device to the bare wind turbine without any change of its main design. Bukala et al. [6] mentioned the effect of the tower height on the performance of small wind turbines. It was found that increasing the tower height for the same wind speed enhances the wind turbine efficiency significantly. Other geometrical parameters that affect the wind turbine performance were described, such as pitch angle, twist angle, tilt angle, turbine size, airfoil shape, and others [7–9]. A pitch angle of 2° has been discovered to be the best angle as it increased the wind turbine coefficient of performance by about 6.6% [7]. It was deduced that the torque generated from the wind turbine is directly proportional to the cube of rotor diameter, while the aerodynamic forces increase with the square of the diameter [9]. New wind turbines designs were proposed and studied for the same purpose of ameliorating their efficiency [10–18]. El-Baz et al. [11] suggested an optimized Savonius wind turbine system design comprising three turbine rotors arranged in a triangular pattern. They found that the performance was improved significantly compared with the single rotor design. Fatehi et al. [10] presented a different airfoil shape by deploying an optimized cavity on it. It was concluded that the blade with cavity could increase the stall angle of attack by 3°. Furthermore, Hashem and Mohamed [12] introduced a research on 24 new straight-bladed Darrieus wind turbine airfoils including symmetric and non– symmetric shapes. It was revealed that the three-bladed Darrieus turbine with S1046 as a sectional profile gives the maximum performance. Govind [19] proposed a different innovation by combining horizontal and vertical axis wind turbines in the same model in order to benefit from the advantages of both wind turbine types and improve the overall performance. On the other hand, some researchers preferred to rely on augmentation devices such as diffuser, guide vanes, stator, shroud, plate, deflector, or duct to enhance the wind turbine efficiency as mentioned previously [14,20–30]. Many research studies [20,23–26] were concerned with diffuser-augmented wind turbines (DAWTs) and they found that the diffuser has a positive effect on the performance of wind turbines, as it concentrates and deflects the wind flow to increase the positive torque and reduce negative torque. Stator vanes have a similar impact on wind turbines performance as described in [27] and [28]. Otherwise, adding a deflector to the conventional wind turbine system was discovered to be a simple way to enhance the coefficient of performance and reduce the negative torque induced from the returning blades as mentioned in the referred studies [14,21,22,29,30]. Moreover, the deflector accelerates the wind flow towards the advancing blades. Golecha et al. [29] and Mohamed et al. [30] aimed to modify the Savonius wind turbine performance with the aid of flat plate deflector. Besides, Golecha et al. [29] investigated the effect of the flat obstacle for single, two, and three stage rotors. Other research studies decided to benefit from the deflector effect from both sides by working on counter-rotating wind turbines model [21,22]. Finally, a new self-orienting curtain system was suggested by Tartuferi et al. [14] and deployed with Savonius wind turbine. The majority of studies regarding the effect of the deflector on the wind turbine performance currently focus on Savonius wind turbines, while Darrieus wind turbine studies are not widespread for this point of research.

The novelty of the presented study is the investigation of changes of the aerodynamic performance of three-bladed H-Darrieus VAWT resulting from adding different plate deflector configurations. In the current study, a 2D transient model, have been investigated to compare and optimize the Darrieus wind rotor performance with and without deflector, in order to maximize the power captured from wind energy. The results will provide wind turbine designers with a method to estimate the performance of VAWT.

2. Problem description and setup

In this study, Finite Volume Fluent Solver has been investigated, using Unsteady Reynolds Averaged Navier Stokes (URANS) governing equations, to capture the effect of different deflector configurations on the aerodynamic performance of vertical axis wind turbine airfoil. A two dimensional, incompressible and turbulent flow model has been represented in the current study.

Table 1 Main geometrical rotor features.

D_{rotor} [mm]	1030
H_{rotor} [m]	1 (2D simulation)
N [-]	3
Blade profile	NACA 0021
c [mm]	85.8
σ [-]	0.5

Where, D_{rotor}, H_{rotor}, N, c and σ are Rotor Diameter, Rotor Height, Number of Rotor Blades, Blade Chord and Rotor Solidity respectively.

This section contains a brief explanation of the procedure used to compute the coefficient of momentum (C_m), followed by the validation of numerical model results against wind tunnel results. Then, the effect of the deflector was analyzed using two different configurations. The two represented deflector designs were single deflector and double deflector with nozzle flow action. These deflector configurations were compared with the case of a bare wind turbine.

2.1. H-Darrieus wind turbine geometry features

Table 1 summarizes the main geometrical features of the Darrieus wind turbine used in this study and described by Castelli et al. [31]. As there are no provided information on the shaft, the CAD of the rotors were simplified eliminating the shaft and representing only the blades.

2.2. Wind turbine governing parameters

The total moment coefficient used in the numerical model is estimated as the sum of moment coefficients of the three blades. The fluctuating moment coefficient values are averaged in order to predict the turbine global efficiency. Being a temporary state, the transient effect must not be taken into account, in the first three cycles, because the solution is not yet stable. Our model validation has been investigated by comparing the coefficient of power (C_p) vs. tip speed ratio (λ) curve with results in the literature. In order to obtain the C_p from the previously computed C_m value, the following equation is used:

$$C_p = C_m(\omega L)/V \quad (1)$$

Where, ω, L and V are Rotor Angular Velocity, Reference Length and Wind Velocity respectively.

When the turbine simulation is 2D, the value of L is equal to the radius of the turbine (R) as described in [32].

By substitution, Eq. (1) becomes:

$$C_p = C_m(\omega R)/V \quad (2)$$

But the equation that describes the tip speed ratio (λ) is:

$$\lambda = (\omega R)/V \quad (3)$$

Then, in order to validate the numerical results, the final equation used to obtain the (C_p) from averaged (C_m) calculated value is:

$$C_p = C_m\lambda \quad (4)$$

2.3. Numerical details and solver setup

As the aim of the present work is the simulation of a turbine operating in open field conditions and because of the huge domain width necessary to avoid solid blockage, inlet and outlet boundary conditions were placed using the presented dimensions in Fig. 1. The computational domain is divided into two parts: A stationary field consisting of the outer domain and a rotating domain containing the turbine blades.

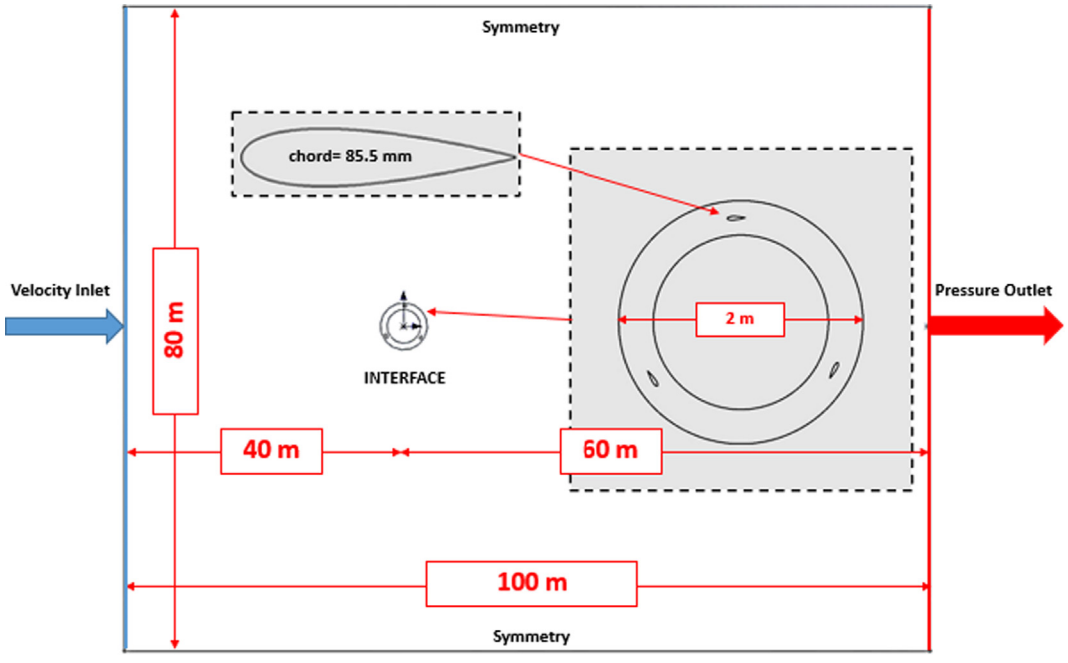

Fig. 1 Computational domain.

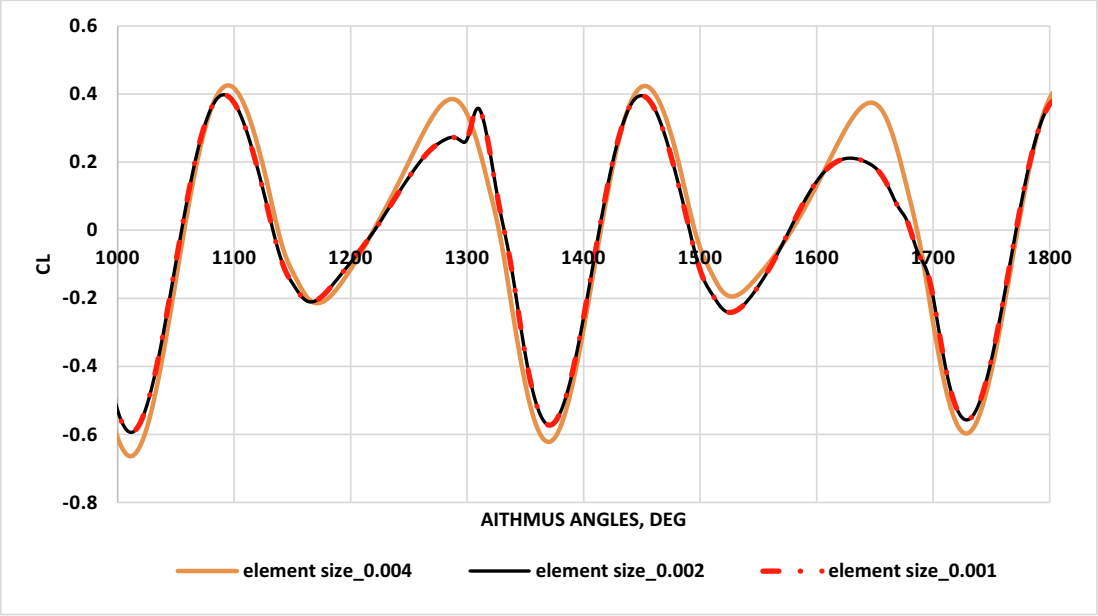

Fig. 2 Mesh Independency Test.

The two domains are coupled together via a sliding mesh technique and linked through "interfaces". Two symmetry boundary conditions were used for the two side walls.

Grid independence has been checked by simulating the VAWT, at wind speed of 9 m/s and tip speed ratio (λ) of 2.51, with three different grids. Coarsening and refinement has been made by halving and doubling the number of elements respectively in all directions, without changing the dimensionless wall distance Y plus. Results for the average power coefficient do not differ for more than 10^{-3} units. For the entire domain, an unstructured mesh composed of triangular elements was used, gradually refining towards the rotor region to capture the development and mixing of the wake behind the rotor. For the blade discretization, on the other hand, an O–grid of quadrilateral elements was used, as shown in Fig. 3, in order to adequately resolve the boundary layer surrounding the airfoil. The intermediate mesh with 650,000 elements has been retained since meets accuracy requirements at an affordable computational cost. The mesh independency and the resulting mesh are shown in Figs. 2 and 3 respectively. The range of values of the dimensionless wall distance Y plus (Y +) through the wind turbine blade airfoils were less than 1. The first grid height around the airfoil is 5.4 μm.

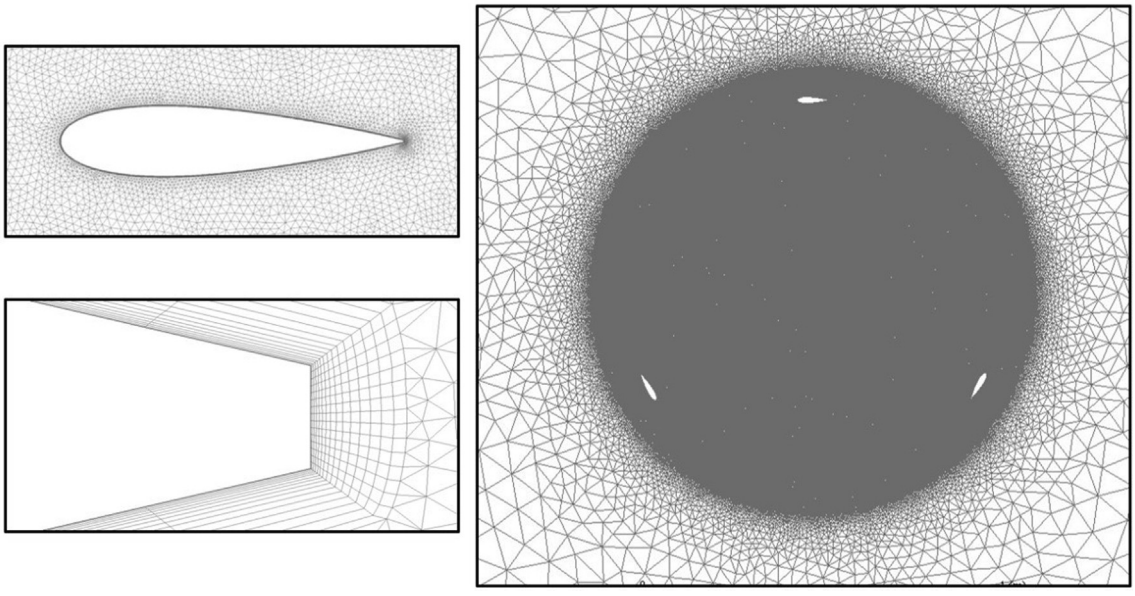

Fig. 3 Grid distribution around one rotor blade.

2.4. Numerical setup

The aerodynamic behavior of the three-bladed Darrieus VAWT was numerically investigated at different angular velocities for a constant wind speed of 9 m/s.

The CFD model used in this study is based on the solution of the two–dimensional unsteady Reynolds Averaged Navier Stokes equations (U–RANS), utilizing k-ω SST model to resolve the turbulent problem. The SIMPLE algorithm is used to solve the coupled velocity–pressure problem. A second-order upwind scheme is used to calculate momentum, turbulence kinetic energy and dissipation ratio. The inlet boundary was set as a velocity-inlet, the outlet boundary was set as a pressure-outlet, and the airfoil surface was set as a wall with no slip.

The time step (Δt) calculation is evidently dependent on the angular velocity of the wind turbine and indicates the number of degrees that the mesh rotates in every calculation [33]. Because of the great variation of angular speed and the complexity of the flow field, it was impossible to find an optimal time step for the transient solver. Above all at high angular speed and high wind speed the time step should be very little to sufficiently simulate rotation and capture the little time scale of turbulence. In addition, the time step impacts the numerical iterative process of the solver, that means that too great a time step leads to unphysical results, while too little a time step leads to great increase in computation time. Basing on these considerations, time step was optimized performing several simulations at different angular speed for both rotors. A first attempt value was fixed considering the angular velocity. Establishing an angular step of 1°, it was calculated the relative time step as follow:

$$\omega = \frac{\Delta \varnothing}{\Delta t} \tag{5}$$

$$\Delta t = \frac{\Delta \varnothing}{\omega} \tag{6}$$

Where, $\varnothing$ is the Deflector Azimuth Angle.

$$\Delta t|1^{\circ} = \frac{1}{360\omega} \tag{7}$$

As these time step values did not meet the convergence criteria and led to bad results compared to experimental data, they were gradually decreased till the solution was converged and the results using two consecutive time steps were negligible. The time step for the current simulation was $\Delta t = 4.274 \times 10^{-4}$ s. This gave a Courante-Friedrichs-Lewy number (CFL) less than 1 for the rotating grid. According to Trivaletto et al. [34], CFL should be less than 0.5 for constant grid spacing, but in most numerical simulations, grid spacing is not constant. It was proved that a linear relation between CFL number and numerical error exists also for meshes with variable sized elements; as the CFL number is reduced, the numerical error points to a minimum value and this is true for 1D and 2D problems alike.

The angle of attack is determined by a simple relationship between the azimuth angle and the speed ratio. It can be calculated as follows [35]:

$$\alpha = \tan^{-1}\left[\frac{\sin(\phi)}{\lambda + \cos(\phi)}\right] \tag{8}$$

2.5. Added deflector configurations

To improve the wind rotor aerodynamic performance, it is important to avoid the negative torque that forms in the adverse direction of the rotor's rotating direction. Two deflector designs have been introduced and investigated for the purpose of increasing the aerodynamic performance of the Darrieus wind rotor without making any modifications in its elementary structure. Figs. 4 and 5 show the single deflector and double deflector with nozzle flow action configurations respectively. In the double barrier arrangement, α-β represents the angles of curtain plates. According to [36], it has been indicated that the best performance for wind rotor is obtained at $\alpha = 80°$ and $\beta = 80°$. Consequently, these angles have been used in the current study.

3. Verification and validation

Firstly, the mesh sensitivity was checked obtaining the minimum number of cells that could be used in the full two-dimensional Navier-Stokes simulation. Secondly, to ensure that the numerical model is suitable for the free-stream flow past the wind turbine rotors, the numerical simulation was compared with the experimental and numerical data presented

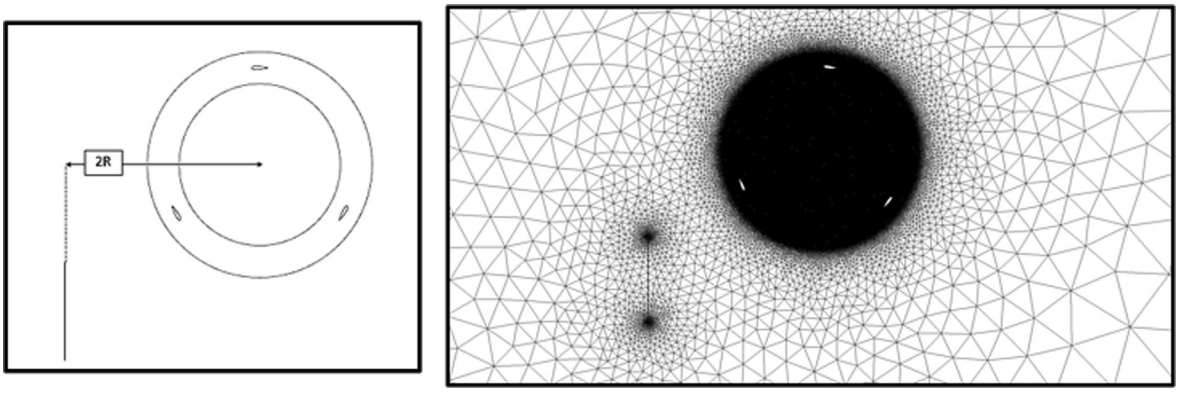

Fig. 4 Single Deflector Configuration Design.

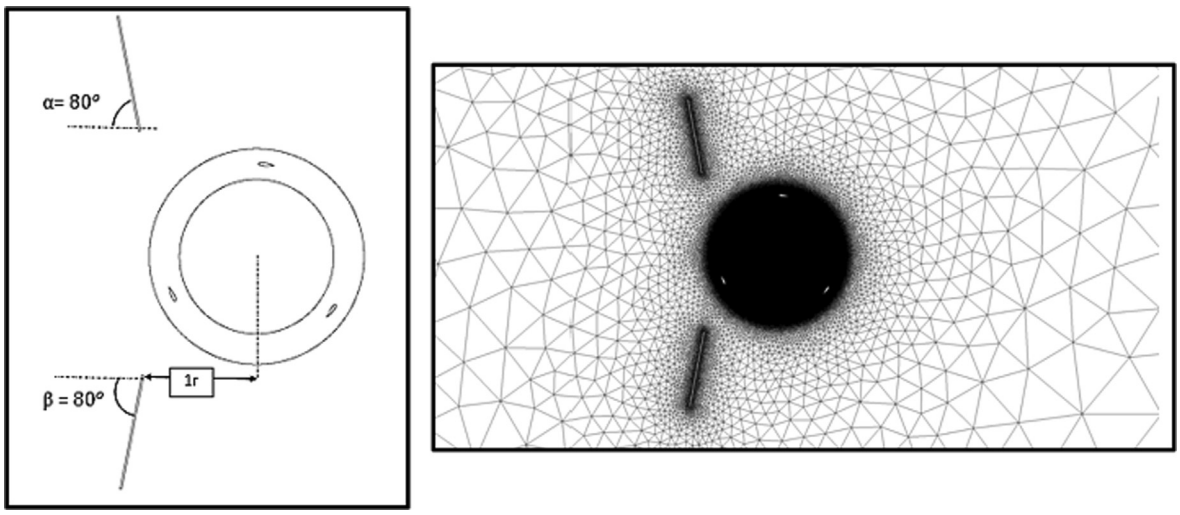

Fig. 5 Double Deflector with Nozzle Flow Action Configuration Design.

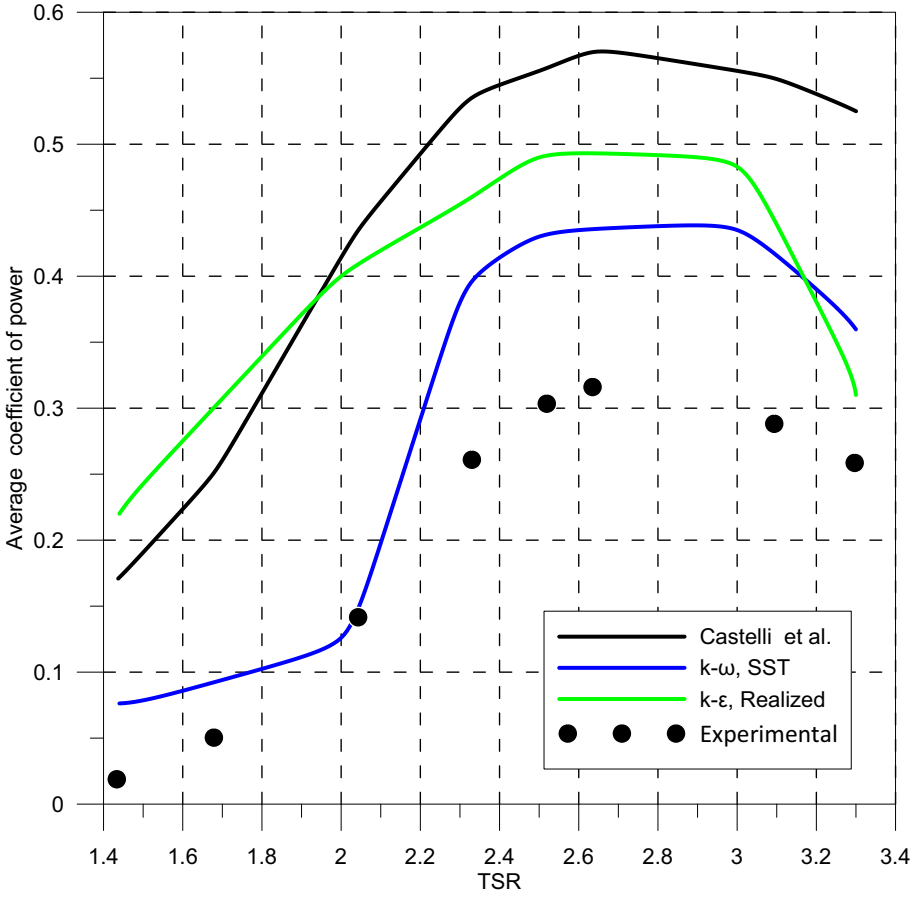

Fig. 6 Comparison between turbulence models.

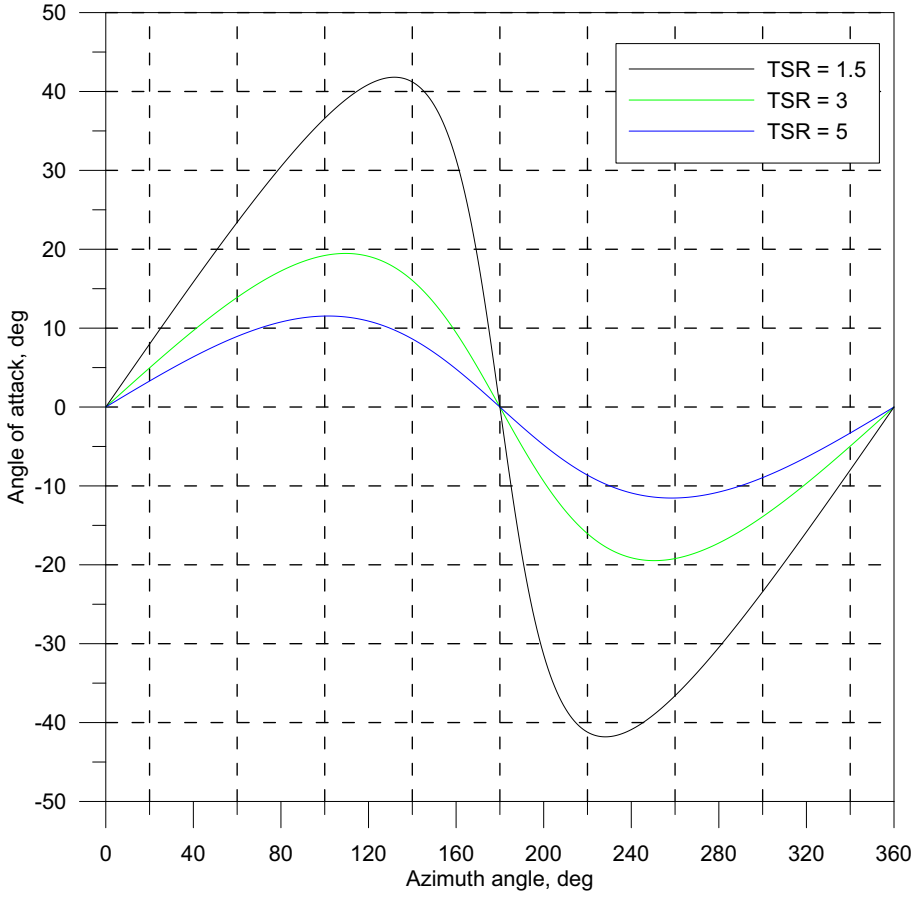

Fig. 7 Angle of attack versus azimuth angle.

by Castelli et al. [31]. The simulative conditions were matched to the wind tunnel set-ups. Wind speed at test section entrance has a value of 9 m/s.

A comparison between the numerical results and the experimental data of the power coefficient (C_p) variation with tip speed ratio (λ) has been investigated using two common turbulence models, used in the previous literature studies [5,31,36], which are Realizable k-ϵ model [37,38] and k-ω SST model [39,40].

As shown in Fig. 6, the numerical results of k-ω SST model provide a reasonable description of the flow at different tip speed ratios considering the losses in the experiments, including wind tunnel blockage [31], have not been taken into account. The results agree with previous comparisons of turbulence models for Darrieus VAWT [30]. Therefore, the k-ω SST model was confirmed to be viable for the free-stream flow past the VAWT airfoils. Despite the observed discrepancy, the numerical and experimental curves have the same trend and the CFD, which improves upon previous CFD results, accurately captures the maximum power coefficient tip speed ratio. There is a consistent difference between the experimental and computational data, which can be attributed to the combined effects of 2-D modelling, hub drag, and wind tunnel blockage [30,31,35].

4. Results and discussion

This section presents the results for three turbine configurations. For each configuration, the moment coefficient was calculated, and flow contours were created to show the effect of the flow deflection on the performance of the turbine.

Fig. 7 shows the fluctuation in angle of attack with azimuthal at different TSR. The peak value of the angle of attack is affected significantly by TSR value and its location is shifted slightly with the increase in TSR. It is observed that the big fluctuation of the angle of attack with variation in azimuth angle. This big fluctuation of angle of attach affects the coefficient of moment and hence the overall performance of the vertical wind turbine. Therefore, it is essential to find a proposed technique to reduce the variation in the angle of attack. This can be achieved by control the wind direction and value using a guide vane or modifying the blade angle. In this study the symmetrical airfoil 0021 was used which has optimum angle

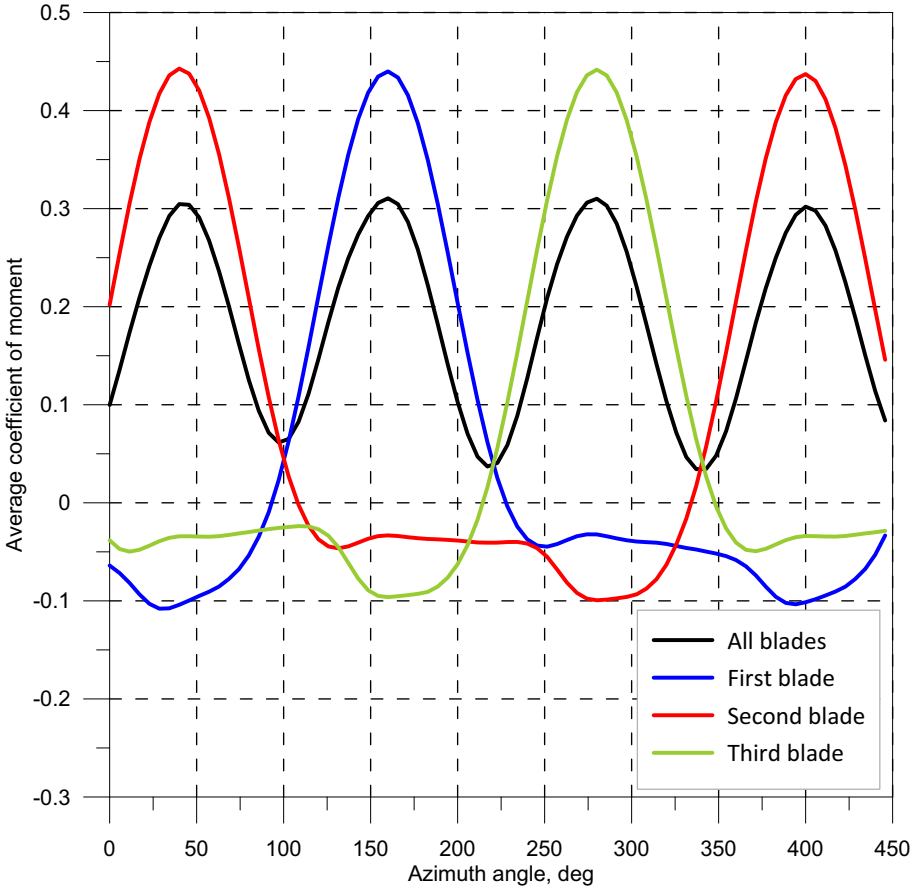

Fig. 8 Numerical moment coefficient of the bare three-blade H-Darrieus turbine.

of attack in range of 10 to 17°. This will explain the poor aerodynamic performance of the bare Darrieus turbine at low TSR which may result in stall at high values of the angle of attack.

For a TSR of 2.5, Fig. 8 shows the moment coefficient fluctuation at different azimuth angles, which are affected by the angle of attack, wind speed and blade rotation speeds. Three peaks are observed for each blade at θ roughly equals to 90°, 210 and 330. This is due to the lift force, which is responsible for the rotation of the blade, increasing with the increase of angle of attack as the blade begins to rotate. However, when the blade chord is perpendicular to the wind flow direction at 90°, the airfoil reaches its maximum or critical angle of attack. From that point, the blade begins to stall, and the lift force faces a big decrease resulting in low coefficient of torque values. However, this is an instantaneous stall, due to the rotational movement of the blade of the VAWT.

Fig. 9 shows the overall average C_m trend against TSR for the three turbine configurations. All configurations result in low C_m at the lower value of TSR which indicates low startup torque by utilizing the Darrieus rotor turbine. As the TSR increases, the C_m increases to a maximum value then decreases again. This is owing to the effect of TSR on the angle of attach as previously shown in Fig. 7. It is observed also in Fig. 9 that the existence of the deflector extends the operation range of the turbine rotor and enhances the performance. The bare Darrieus has reached a maximum moment coefficient at a TSR of 2.6, while the turbine with a single deflector achieved its peak value at TSR of 3.1, and the turbine with 2 deflectors reached its optimum value at TSR of 3.3, which is the best of the three configurations. This results from the enhancement in the aerodynamics performance by implementing the directional guide vane, which will be discussed later.

Fig. 10 shows the variation of the 3-blade average C_m with the azimuth angle for the three turbine configurations at a TSR of 3.3. As a result of flow deceleration in front of the flat plate deflector, a low velocity zone has been created, which leaded to blockage effects. The wind flow was then separated and deflected to the top and the bottom, which resulted in high vortices wake region being created downstream the deflector. Another important function of the deflector is that it accelerates the wind flow significantly when the wind hits it at its top and bottom. While using a single deflector increases the maximum torque value due to the increase in the flow velocity flowing over the blade, it has an adverse effect on the negative torque. Utilizing two deflectors upstream of the turbine rotor overcomes this drawback by blocking the flow in the zone where the rotor blade rotates opposite to wind direction and

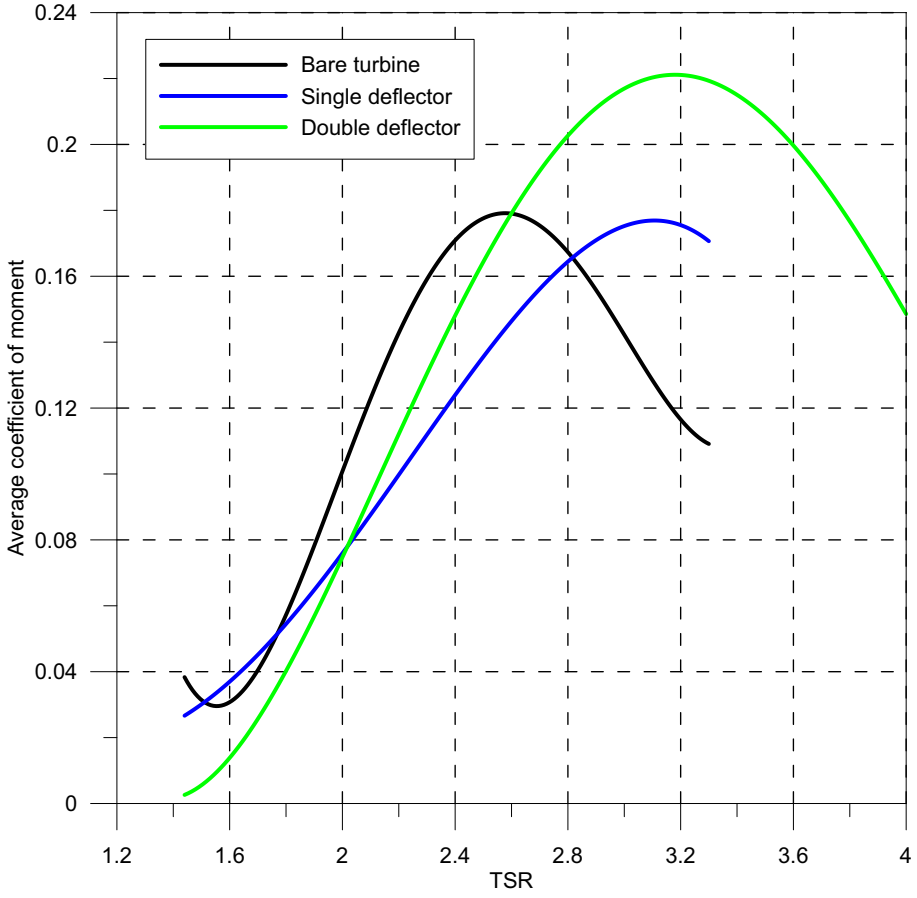

Fig. 9 Numerical moment coefficient of three-blade H-Darrieus turbines comparing aerodynamic performance of bare, single and double deflectors.

concentrating the flow in the zone where the preferable angles of attack occur.

The overall result is a higher maximum coefficient of momentum for both the single and double deflector configurations compared to the bare turbine. The single deflector configuration has the disadvantage of some azimuthal angles with a negative coefficient of momentum, but these are eliminated with the double deflector configuration. The results for the coefficient of momentum are reflected in the calculated torque, which is discussed below.

Table 2 compares the values of forces and torque at different azimuth angle for all turbine configurations at TSR of 3.3. For all configurations, the worst zone was located from 0 to 30°, and the crest torque value range is located from 60 to 120°. When the blade passes through the downstream region, the pressure difference between the inner and the outer surfaces of the blade becomes smaller than in the upstream region. This is due to the dissipation of wind energy in the downwind zone of the turbine. Consequently, the torque created in the upwind region becomes much greater that the downwind region.

Adding one deflector in front of the turbine rotor increase the positive torque in the co-rotating zone due to the creation of the wake behind the deflector, which causes the flow to accelerate toward the blades in the potential zone. However, the presence of the deflector results in more reduction in torque in the counter-rotating zone for the same reason.

Inserting two deflectors upstream of the turbine rotor results in one wake behind each deflector which generate a nozzle action in between the two wake zones. This situation has a positive effect on both counter-rotating and co-rotating zones as shown from Table 2 and Fig. 11. The range of angles with negative torque is also reduced for the double deflector configuration compared to the other configurations.

The previous results can be observed emphatically in the streamlines results, which are depicted in Fig. 12. The maximum velocity increases for the single and double deflector configuration compared to the bare turbine. This increase in velocity is responsible for an increase in lift resulting in the increase in coefficient of momentum and maximum torque seen earlier. The increase in maximum velocity would also be expected to lead to an increase in drag, but this is mitigated by the effects of the deflectors on the transitional separation bubble as discussed below.

According to the study presented by [41], a transitional separation bubble occurs when the boundary layer separates from

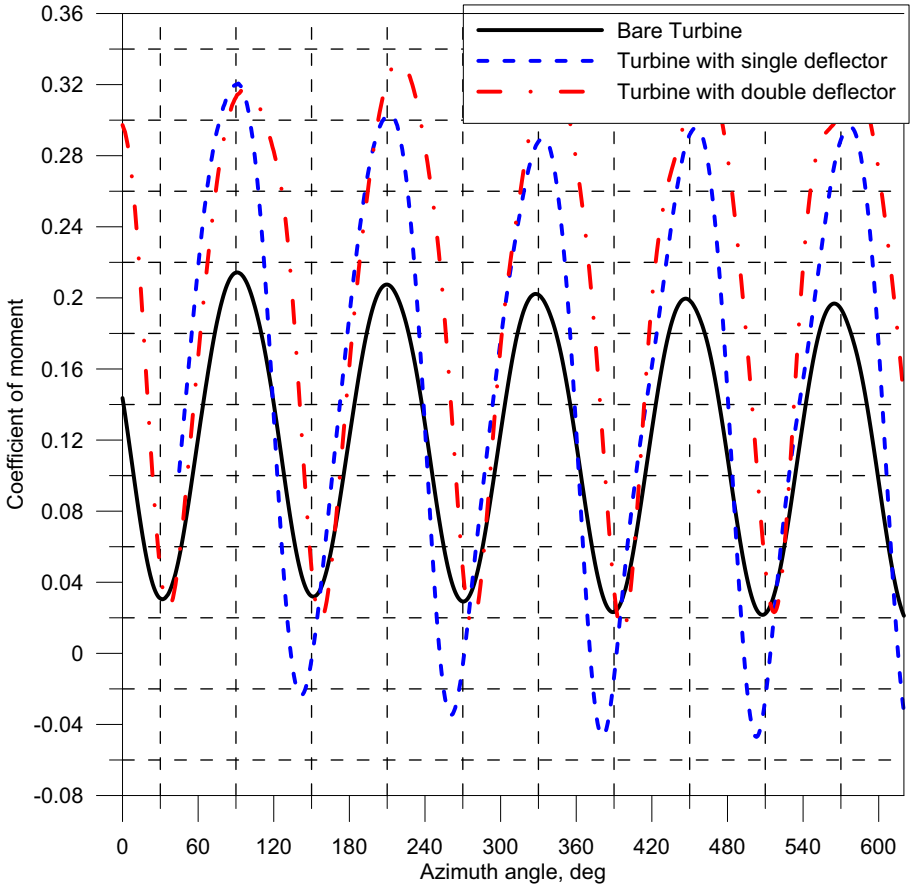

Fig. 10 Variation of C_m with the azimuth angle for the three turbine configurations at TSR of 3.3.

Table 2 Effect of azimuth angle on a single blade forces and torque values at TSR = 3.3.

Azimuth Angle	Bare Turbine			With single deflector			With double deflector		
	Fx	Fy	Moment	Fx	Fy	Moment	Fx	Fy	Moment
0	0.5	9.63	−0.5	−0.05	9.05	−0.57	−1.2	16.26	−0.28
30	6.78	−9.8	−0.75	12.8	−19.13	−0.32	15.16	−23	−0.17
60	39.2	−27.4	1.79	49.19	−33.37	3.6	53.4	−36.8	4.45
90	57.6	−9.44	4.6	76.9	−12.2	7.72	66.36	−10	6.9
120	42.9	14.9	4	33.3	12.35	4.08	45.6	16.96	5.5
150	12.47	17	1	−5.5	−10	−0.18	3.35	6.32	0.08
180	−0.44	−1.54	−0.3	1.52	−12.85	0.19	3.5	−21	1.11
210	6.9	−10.35	0.2	2.13	−3.7	−0.33	3.46	−4.8	−0.16
240	9.54	−5	−0.003	7.35	−0.4	−0.2	10	−4.36	0.11
270	12.45	0.4	0.02	14.25	1.57	0.15	23	4	1.12
300	13.8	8.9	0.2	15.86	12.04	0.48	21.2	17.9	1.39
330	8.57	16.6	0.16	8.6	19.52	0.37	9.8	25.34	0.97
360	0.48	8.2	−0.5	0.157	8.83	−0.57	−0.65	12.5	−0.38

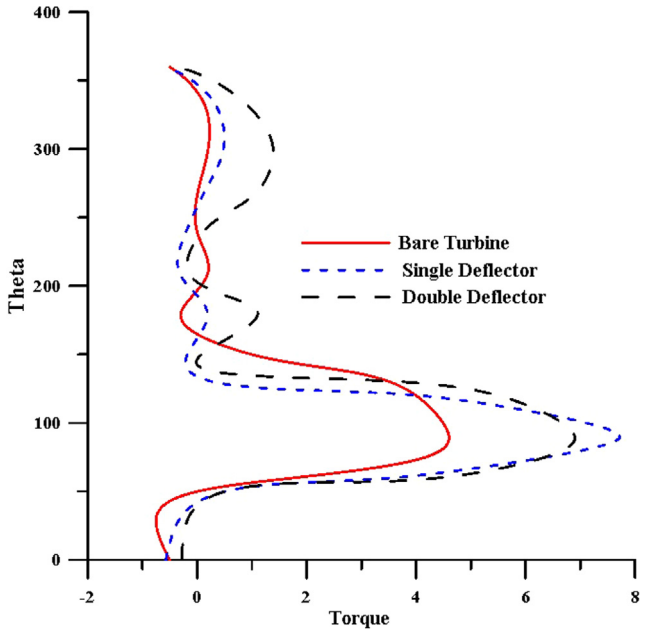

Fig. 11 Variation of the azimuth angle with generated torque for the three turbine configurations at TSR of 3.3.

the airfoil surface due to an adverse pressure gradient. Figs. 13, 14 and 15 describe the flow separation phenomenon occurred before and after adding different wind rotor barriers at AOA 0°, 90°, 180° and 270° respectively. These velocity contours have been represented at optimum TSR values, which obtain maximum power coefficient for each configuration. The optimum TSR value before adding the deflectors is 2.3. However, the optimum TSR value after adding the two deflector configurations is 3.3. After the laminar boundary layer separation, a highly unstable detached shear layer forms and transition to turbulence takes place in the detached shear layer. The enhanced momentum transport in the turbulent flow enables reattachment and a turbulent boundary layer develops downstream. The separation bubble thickens the boundary layer and thus increases the pressure drag of the airfoil. The drag increase can be several times the drag of the airfoil without a separation bubble. In addition, lift is influenced by a transitional separation bubble, which can lead to problems with the aerodynamic performance of the airfoil. According to the figures shown, increasing angle of attack causes boundary layer separation to occur further upstream and produce a shorter transitional separation bubble. However, due to the addition of the wind rotor barriers, the height and length of the transitional separation bubble decreased. As a result, the aerodynamic performance of the VAWT increased.

5. Conclusion

The current study has shown the benefits of employing a deflector upstream of the H-Darrieus turbine. The performance of the H-Darrieus turbine was investigated using Ansys Fluent CFD software with and without upstream deflectors. The following summarizes the main results of the current work:

- At low TSR, both the moment and power coefficients are low, and the presence of defectors has little impact.
- The turbine with a single deflector has a negative effect on the moment coefficient approximately up to TSR = 2.8. Although it increases the flow momentum into the potential co-rotating zone, it has an adverse effect on the flow in the counter rotating zone
- Due to the nozzle action created by the two deflectors, it results in approximately a 22% increase in the average moment coefficient over the bare H-Darrieus. In addition, it expands the turbines operating range approximately to TSR = 3.2.
- The presence of defectors influences the maximum and lowest values of the moment coefficients but not their position.

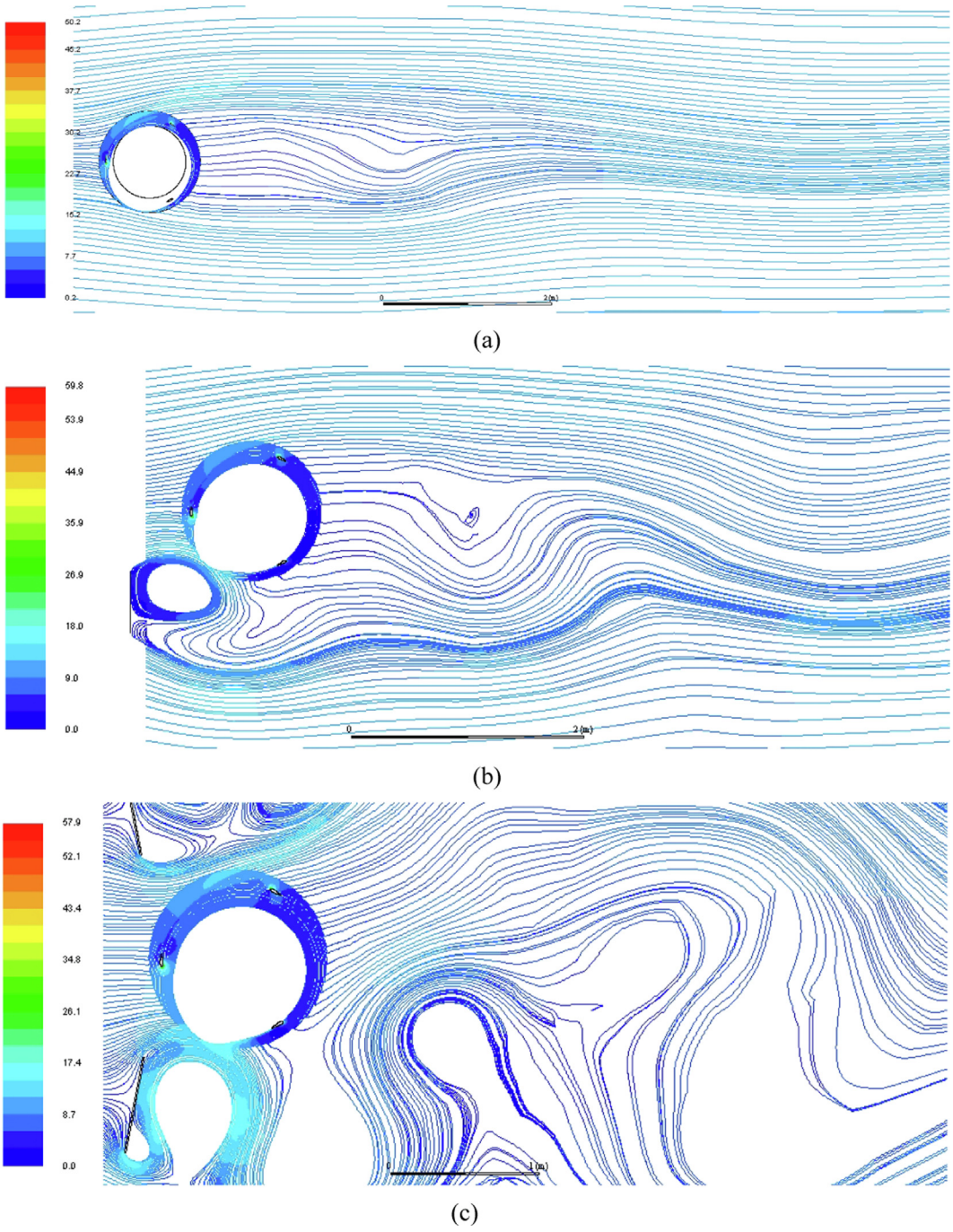

Fig. 12 Streamlines colored by velocity magnitude for a. bare rotor b. rotor with single deflector c. rotor with two deflectors at TSR = 3.3.

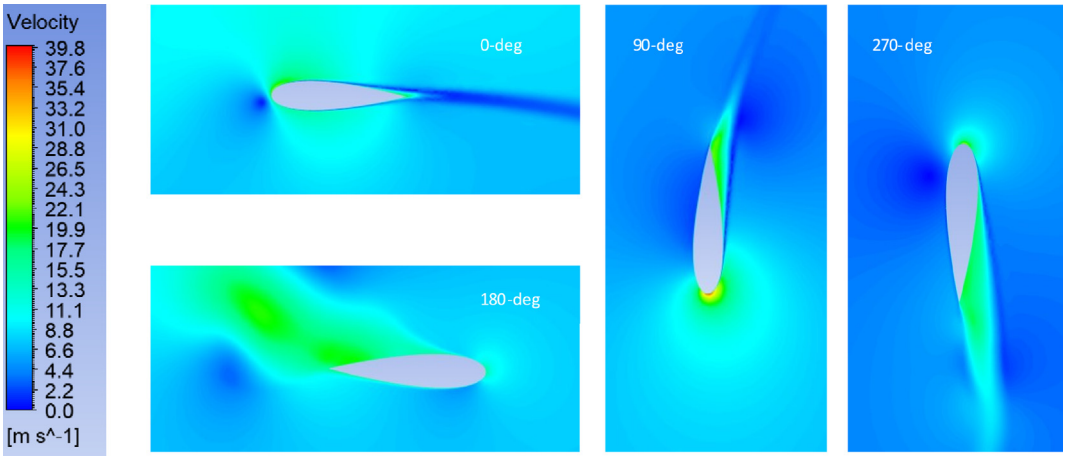

Fig. 13 Velocity contours for bare rotor at its optimum TSR = 2.3 showing the transitional separation bubble.

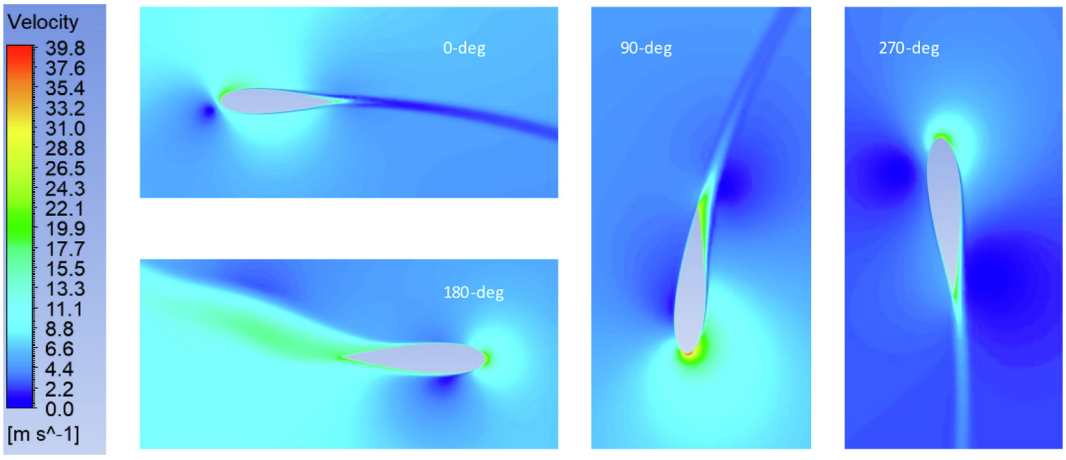

Fig. 14 Velocity contours for rotor with single deflector at its optimum TSR = 3.3 showing the transitional separation bubble.

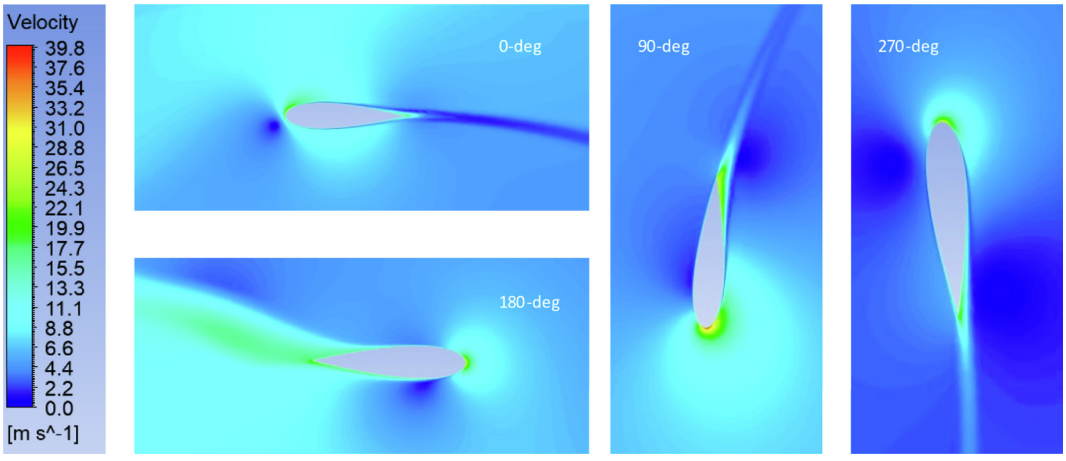

Fig. 15 Velocity contours for rotor with two deflectors at its optimum TSR = 3.3 showing the transitional separation bubble.

Declaration of Competing Interest

The authors declare that they have no known competing financial interests or personal relationships that could have appeared to influence the work reported in this paper.

References

[1] I.F. Zidane, K.M. Saqr, G. Swadener, X. Ma, M.F. Shehadeh, On the role of surface roughness in the aerodynamic performance and energy conversion of horizontal wind turbine blades: a review, Int. J. Energy Res. 40 (15) (2016) 2054–2077.
[2] I.F. Zidane, G. Swadener, X. Ma, M.F. Shehadeh, M.H. Salem, K.M. Saqr, Performance of a wind turbine blade in sandstorms using a CFD-BEM based neural network, J. Renew. Sustain. Energy 12 (5) (2020) 053310.
[3] M. Kalantar, Dynamic behavior of a stand-alone hybrid power generation system of wind turbine, microturbine, solar array and battery storage, Appl. Energy 87 (10) (2010) 3051–3064.
[4] S. Soua, P. Van Lieshout, A. Perera, T.-H. Gan, B. Bridge, Determination of the combined vibrational and acoustic emission signature of a wind turbine gearbox and generator shaft in service as a pre-requisite for effective condition monitoring, Renew. Energy 51 (2013) 175–181.
[5] R. Lanzafame, S. Mauro, M. Messina, 2D CFD modeling of H-Darrieus wind turbines using a transition turbulence model, Energy Procedia 45 (2014) 131–140.
[6] J. Bukala, K. Damaziak, K. Kroszczynski, M. Krzeszowiec, J. Malachowski, Investigation of parameters influencing the efficiency of small wind turbines, J. Wind Eng. Ind. Aerodyn. 146 (2015) 29–38.
[7] A. Rezaeiha, I. Kalkman, B. Blocken, Effect of pitch angle on power performance and aerodynamics of a vertical axis wind turbine, Applied Energy 197 (2017) 132–150.
[8] J.-H. Lee, Y.-T. Lee, H.-C. Lim, Effect of twist angle on the performance of Savonius wind turbine, Renew. Energy 89 (2016) 231–244.
[9] M.H. Giahi, A. Jafarian Dehkordi, Investigating the influence of dimensional scaling on aerodynamic characteristics of wind turbine using CFD simulation, Renew. Energy 97 (2016) 162–168.
[10] M. Fatehi, M. Nili-Ahmadabadi, O. Nematollahi, A. Minaiean, K.C. Kim, Aerodynamic performance improvement of wind turbine blade by cavity shape optimization, Renew. Energy 132 (2019) 773–785.
[11] A.R. El-Baz, K. Youssef, M.H. Mohamed, Innovative improvement of a drag wind turbine performance, Renew. Energy 86 (2016) 89–98.
[12] I. Hashem, M.H. Mohamed, Aerodynamic performance enhancements of H-rotor Darrieus wind turbine, Energy 142 (2018) 531–545.
[13] G. Bedon, S. De Betta, E. Benini, Performance-optimized airfoil for Darrieus wind turbines, Renew. Energy 94 (2016) 328–340.
[14] M. Tartuferi, V. D'Alessandro, S. Montelpare, R. Ricci, Enhancement of Savonius wind rotor aerodynamic performance: a computational study of new blade shapes and curtain systems, Energy 79 (2015) 371–384.
[15] F. Balduzzi, A. Bianchini, R. Maleci, G. Ferrara, L. Ferrari, Critical issues in the CFD simulation of Darrieus wind turbines, Renew. Energy 85 (2016) 419–435.
[16] A. Rezaeiha, I. Kalkman, B. Blocken, CFD simulation of a vertical axis wind turbine operating at a moderate tip speed ratio: guidelines for minimum domain size and azimuthal increment, Renew. Energy 107 (2017) 373–385.
[17] F. Bianchini, G. Balduzzi, L. Ferrara, G. Ferrari, V.D. Persico, L. Battisti, Detailed analysis of the wake structure of a straight-blade H-Darrieus wind turbine by means of wind tunnel experiments and computational fluid dynamics simulations, J. Eng. Gas Turbines Power 140 (3) (2018) 032604.
[18] A. Bianchini, F. Balduzzi, G. Ferrara, G. Persico, V. Dossena, L. Ferrari, A Critical analysis on low-order simulation models for Darrieus Vawts: how much do they pertain to the real flow?, J Eng. Gas Turbines Power 141 (1) (2019).
[19] B. Govind, Increasing the operational capability of a horizontal axis wind turbine by its integration with a vertical axis wind turbine, Appl. Energy 199 (2017) 479–494.
[20] F. Sorribes-Palmer, A. Sanz-Andres, L. Ayuso, R. Sant, S. Franchini, Mixed CFD-1D wind turbine diffuser design optimization, Renew. Energy 105 (2017) 386–399.
[21] D. Kim, M. Gharib, Efficiency improvement of straight-bladed vertical-axis wind turbines with an upstream deflector, J. Wind Eng. Ind. Aerodyn. 115 (2013) 48–52.
[22] X. Jin, Y. Wang, W. Ju, J. He, S. Xie, Investigation into parameter influence of upstream deflector on vertical axis wind turbines output power via three-dimensional CFD simulation, Renew. Energy 115 (2018) 41–53.
[23] U. Göltenbott, Y. Ohya, S. Yoshida, P. Jamieson, Aerodynamic interaction of diffuser augmented wind turbines in multi-rotor systems, Renew. Energy 112 (2017) 25–34.
[24] J.R.P. Vaz, D.H. Wood, Aerodynamic optimization of the blades of diffuser-augmented wind turbines, Energy Convers. Manage. 123 (2016) 35–45.
[25] A.M. El-Zahaby, A.E. Kabeel, S.S. Elsayed, M.F. Obiaa, CFD analysis of flow fields for shrouded wind turbine's diffuser model with different flange angles, Alexandria Eng. J. 56 (1) (2017) 171–179.
[26] J.R.P. Vaz, D.H. Wood, Effect of the diffuser efficiency on wind turbine performance, Renew. Energy 126 (2018) 969–977.
[27] K. Pope, V. Rodrigues, R. Doyle, A. Tsopelas, R. Gravelsins, G. F. Naterer, E. Tsang, Effects of stator vanes on power coefficients of a zephyr vertical axis wind turbine, Renew. Energy 35 (5) (2010) 1043–1051.
[28] R. Nobile, M. Vahdati, J.F. Barlow, A. Mewburn-Crook, Unsteady flow simulation of a vertical axis augmented wind turbine: a two-dimensional study, J. Wind Eng. Ind. Aerodyn. 125 (2014) 168–179.
[29] K. Golecha, T.I. Eldho, S.V. Prabhu, Influence of the deflector plate on the performance of modified Savonius water turbine, Appl. Energy 88 (9) (2011) 3207–3217.
[30] M.H. Mohamed, G. Janiga, E. Pap, D. Thévenin, Optimal blade shape of a modified Savonius turbine using an obstacle shielding the returning blade, Energy Convers. Manage. 52 (1) (2011) 236–242.
[31] M. Raciti Castelli, A. Englaro, E. Benini, The Darrieus wind turbine: Proposal for a new performance prediction model based on CFD, Energy 36 (8) (2011) 4919–4934.
[32] Vaishnav, E., *An Investigation on the Aerodynamic Performance of a Vertical Axis Wind Turbine*. 2010.
[33] F. Balduzzi, A. Bianchini, G. Ferrara, L. Ferrari, Dimensionless numbers for the assessment of mesh and timestep requirements in CFD simulations of Darrieus wind turbines, Energy 97 (2016) 246–261.
[34] F. Trivellato, M.R. Castelli, On the CourantеFriedrichseLewy criterion of rotating grids in 2D vertical-axis wind turbine analysis, Renew. Energy 62 (2014) 53–62.
[35] F. Alqurashi, M.H. Mohamed, Aerodynamic Forces Affecting the H-Rotor Darrieus Wind Turbine, Model. Simulat. Eng. 2020 (2020) 1–15.
[36] T.G. Abu-El-Yazied, H.N. Doghiem, A.M. Ali, I.M. Hassan, Investigation of the aerodynamic performance of darrieus vertical axis wind turbine, J. Eng. (IOSRJEN) 4 (5) (2014) 18–29.
[37] V. Yakhot, S.A. Orszag, S. Thangam, T.B. Gatski, C.G. Speziale, Development of turbulence models for shear flows by

a double expansion technique, Physics of Fluids A 4 (7) (1992) 1510–1520.
[38] Choudhury, D., *Introduction to the renormalization group method and turbulence modeling*. 1993: Fluent Incorporated.
[39] F.R. Menter, Zonal two equation k-turbulence models for aerodynamic flows, AIAA paper 2906 (1993) 1993.
[40] F.R. Menter, Two-equation eddy-viscosity turbulence models for engineering applications, AIAA J. 32 (8) (1994) 1598–1605.
[41] I. Zidane, G. Swadener, K. Saqr, M. Xianghong, M.F. Shehadeh, CFD Investigation of Transitional Separation Bubble Characteristics on NACA 63415 Airfoil at Low Reynolds Numbers in Proceedings of the 25th UKACM Conference on Computational Mechanics, University of Birmingham, United Kingdom, 2017.